

# Marine EM techniques for gas-hydrate detection and hazard mitigation

KAREN WEITEMEYER, STEVEN CONSTABLE, and KERRY KEY, Scripps Institution of Oceanography, USA

Marine controlled-source electromagnetic (CSEM) sounding is a new tool available to geophysicists for offshore hydrocarbon exploration. Although the technique has been developed for the detection of deep hydrocarbon reservoirs with relatively high resistivities, it also has the potential to be a useful tool for geohazard mitigation via gas hydrate detection. The hydrate target occurs in the shallow section (hundreds of meters in depth), and is manifested by subtle resistivity contrasts (a few  $\Omega\text{-m}$ ). This requires modifications to the CSEM technique to extend its capability of imaging the shallower hydrate section.

**Motivation.** Marine gas hydrates can be a problem for development and production when working in the hydrate stability regime (high pressures and cool temperatures), possibly resulting in production delays and “blowouts” of wells. In addition, hydrates can contribute to slope instability, which may threaten seafloor infrastructure. The detection of hydrates other than by direct sampling is difficult. Often a seismic signature, called the bottom-simulating reflection (BSR), will mark the bottom of a hydrate layer where solid hydrate exists above and free gas exists below. While seismic methods may be able to detect this lower stratigraphic bound of the hydrate, there is no seismic reflection from the diffuse upper bound, and there is no seismic signature from within the hydrate volume. Furthermore, in many places such as the Gulf of Mexico, hydrates are known to exist but exhibit no BSR.

Another technique for hydrate detection includes electrical resistivity measurements. Electrical resistivity measurements made in well logs characterize a region containing hydrate as more resistive when compared to background sediment without hydrate. However, well logs only provide point measurements and give no insight into the lateral distribution of hydrate over large areas. Even drilling multiple holes provides little indication of the large-scale distribution of hydrate. Needless to say, drilling is expensive and drilling into hydrates can be hazardous, destabilizing hydrate and changing the natural in-situ conditions. A technique is needed to understand the bulk distribution of hydrate on a regional scale. The resistivity contrast between hydrate and back-

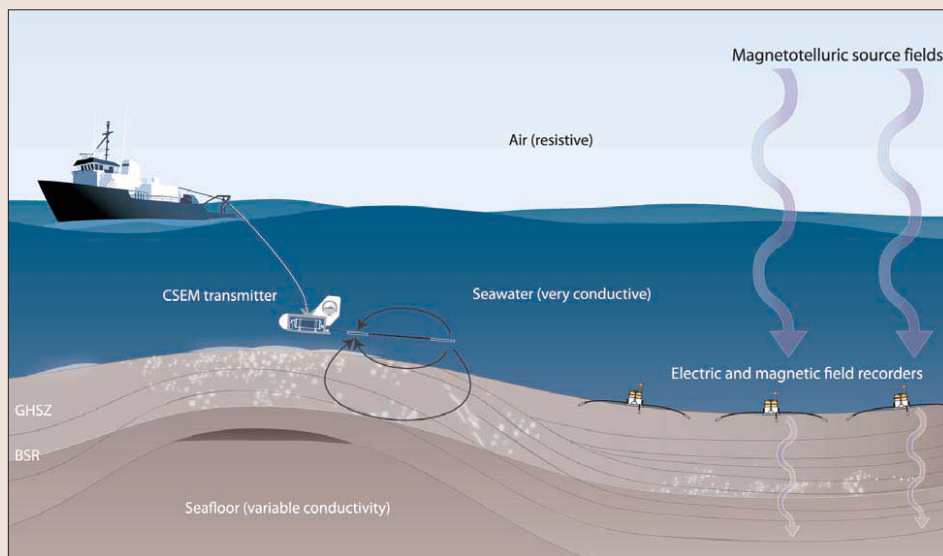
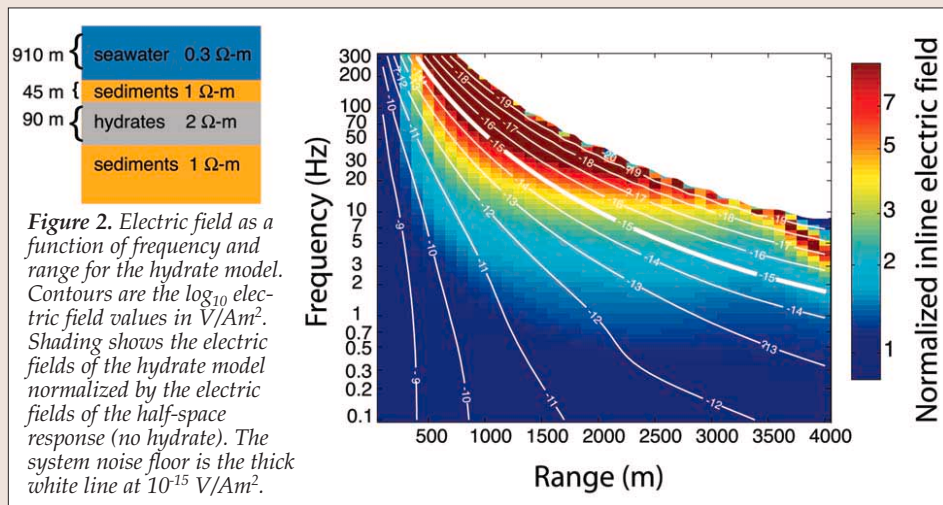


**Figure 1.** For CSEM surveys, an electric dipole transmitter is towed above the seafloor (~100 m) and an alternating electromagnetic field is transmitted along the antenna, which can be 100–200-m long. Seafloor receivers record the electric fields (and magnetic fields) from the transmitter. For the magnetotelluric (MT) method, the same seafloor receivers can be used to record the earth’s time-varying magnetic fields along with induced electric fields. From these an electromagnetic impedance can be computed and, in turn, a large-scale geologic structure is imaged. BSR = bottom simulating reflection; GHSZ = gas-hydrate stability zone.



ground sediment provides an electromagnetic (EM) target, suggesting the use of electromagnetic methods such as CSEM.

Nigel Edwards and his group at the University of Toronto first suggested EM techniques for hydrate detection and have conducted a few studies on the Cascadia margin off the coast of Vancouver Island, British Columbia, Canada, using a towed transient EM system. We have recently used frequency domain CSEM in a pilot study to detect gas hydrate at Hydrate Ridge, offshore Oregon.

**The marine CSEM method.** The CSEM technique used in industry is a frequency domain technique whereby a horizontal electric dipole is towed on or close to the seafloor and

receivers record the transmitted fields at various frequencies and ranges. Electric fields at the receivers are larger over resistive seafloor structures such as hydrocarbon reservoirs or, in this case, gas hydrates. CSEM allows for a noninvasive survey of an area and provides extensive lateral coverage. The CSEM technique can be modified from imaging deep targets to imaging shallow targets by using higher transmission frequencies and collecting data at shorter ranges (shown in Figure 1).

**Modification for hydrate mapping.** The adaptation necessary to use CSEM in the shallow section can be illustrated using 1D forward-modeling studies (Figure 2). Here we model radial mode (transmitter and receiver are in-line) electric fields. We consider a 910-m seawater depth appropriate for our Hydrate Ridge survey area, and a 90-m thick hydrate layer with a resistivity of  $2 \Omega\text{-m}$  at a depth of 45 m below the seafloor in sediment with a background resistivity of  $1 \Omega\text{-m}$ . A 1D model of the electric fields expected from this type of target is normalized by the half-space response with no hydrate. The largest signal from hydrate occurs at ranges and frequencies that current CSEM systems cannot measure—this is shown in Figure 2 as the ranges on and to the right of the thick white line at  $\sim 10^{-15} \text{ V/Am}^2$ , which is the instrument system noise floor. Despite this, a large hydrate signal is detectable at high frequencies ( $> 10 \text{ Hz}$ ) and short ranges ( $< 2000 \text{ m}$ ).

However, the electric fields attenuate very quickly at these high frequencies and have a low signal-to-noise ratio, further limiting the practicality of this bandwidth. In general, high frequencies and short ranges are best to distinguish the top of hydrate, whereas low frequencies and long ranges will discriminate the bottom of hydrate. An increase in hydrate concentration will be reflected by a larger electromagnetic signal and consequently higher electric fields across all frequencies and ranges. There is a trade-off between the large signal from hydrate observed at high frequencies and short ranges and the subtler signal observed at lower frequencies and longer ranges.

Ideally, we want to use a wide-frequency spectrum and collect data over a wide window of ranges to detect all aspects of the hydrate response. This can be partly accomplished by transmitting a square wave, which generates a fundamental harmonic and several odd harmonics, and then choosing the lowest fundamental frequency that has sensitivity to the hydrate layer. In the example (shown in Figure 2), choosing 5 Hz as a fundamental transmission frequency will detect hydrate out to about 3000 m, and the odd harmonics of 15, 25, and 35 Hz will detect the larger signal from hydrate at shorter ranges ( $< 1700 \text{ m}$ ).

A horizontal slice along the 5 Hz frequency-range space in Figure 2 will give electric field magnitudes versus range.

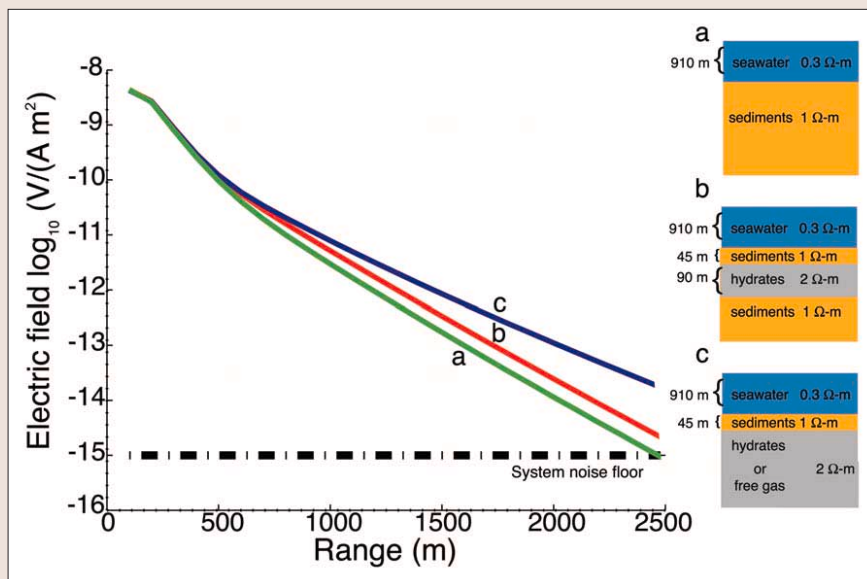


Figure 3. Electric field attenuation for three resistivity models; uniform sediments, a thin hydrate layer, and a thick hydrate layer at a frequency of 5 Hz.

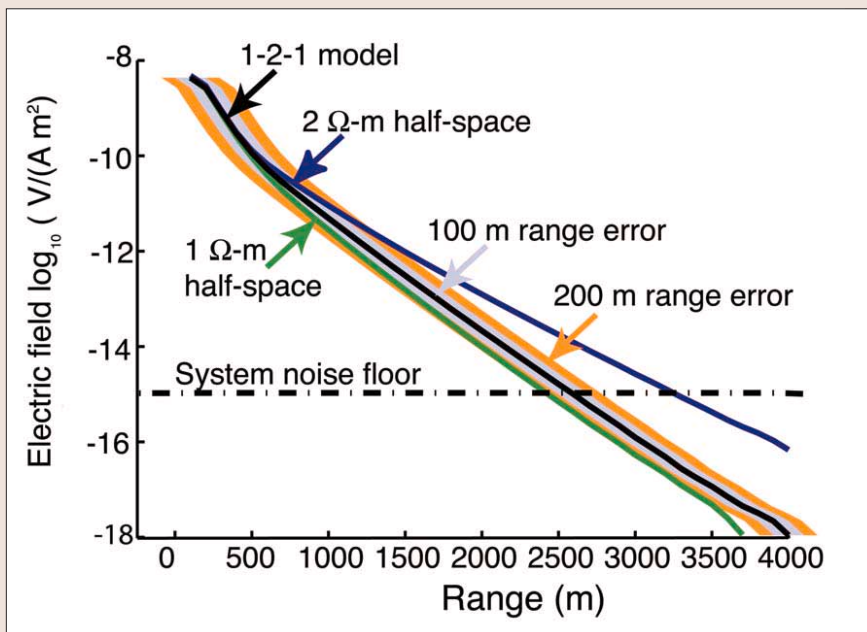
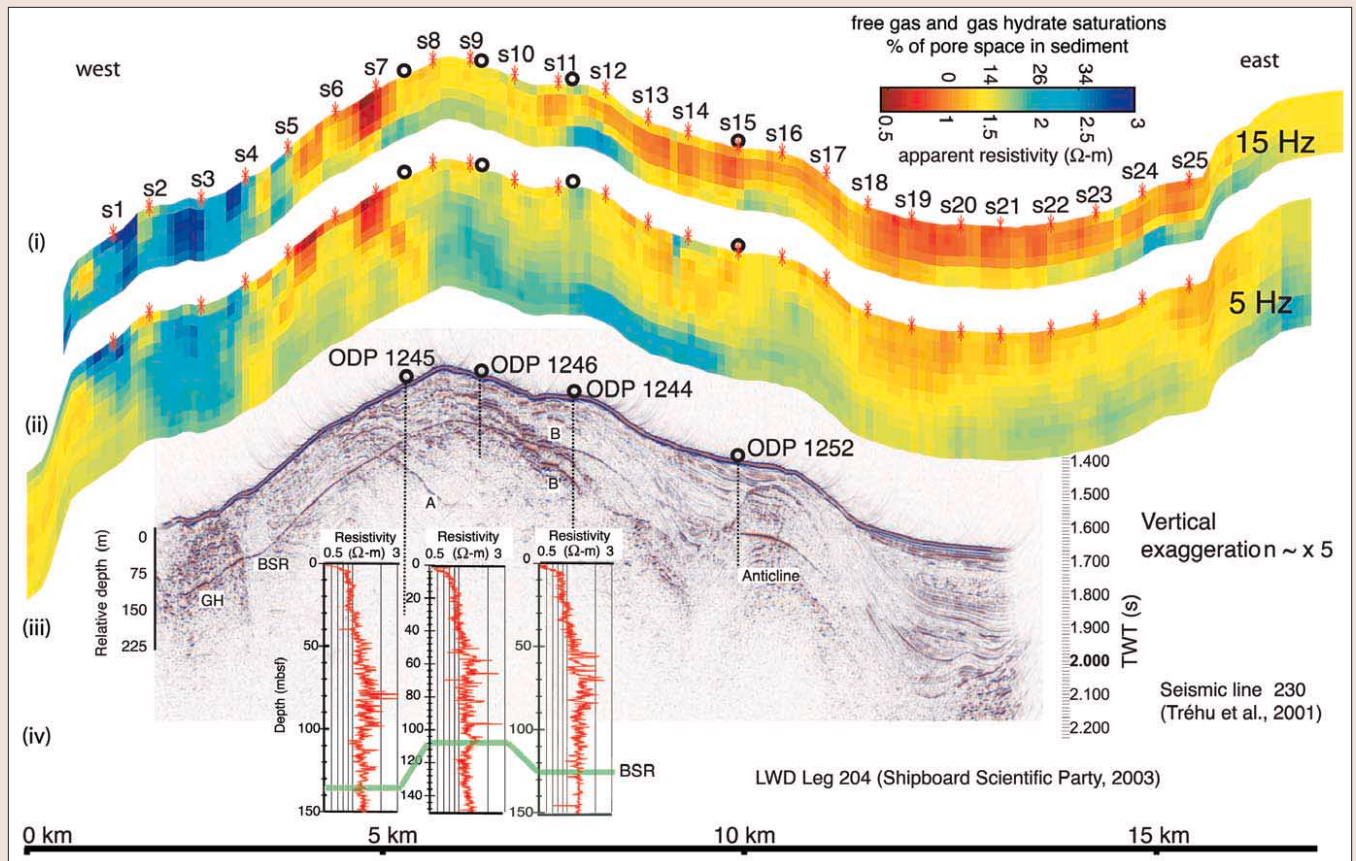


Figure 4. The effect of a 100-m (gray) and a 200-m (orange) error in source-receiver offset (range) results in the measured electric fields appearing stronger or weaker than expected. Here we show the 5-Hz electric fields for 1- $\Omega\text{-m}$  (green) and 2- $\Omega\text{-m}$  (blue) half-spaces and the hydrate layer model (black).

This is shown in Figure 3 for three models—sediment, a thin hydrate layer, and a thick hydrate layer. Each model creates different electric field attenuation as the source-receiver range increases. The largest signal comes from the thick hydrate layer, while the weakest signal is from the sediment half-space. The model study shows that CSEM can measure the existence and thickness of the modeled hydrate layer.

**Pitfalls.** Navigation errors are more significant at short ranges than at long ranges, so navigation plays a key component in gas-hydrate detection because of the short ranges used. Figure 4 shows a 2- $\Omega\text{-m}$  and 1- $\Omega\text{-m}$  half-space response for electric field versus range. It also shows the electric field magnitudes for the hydrate model, which falls between the 1- and 2- $\Omega\text{-m}$  half-space responses. Included are the error bands showing 100 m and 200 m range errors in the hydrate response—100 m



**Figure 5.** (i) 15- and (ii) 5-Hz data in pseudosection form with a combined apparent resistivity and gas-hydrate saturation scale linked through Archie's law; (iii) seismic line 230, and (iv) logging-while-drilling (LWD) deep resistivity logs. GH = gas hydrate or free gas inferred from a seismic inversion (Zhang et al., 2003); BSR = bottom-simulating reflection; A, B, B' = seismic horizons explained in text. ODP Leg 204 sites are marked on seismic section. EM receiver sites are marked by red asterisk (modified from Weitemeyer et al., 2006).

and 200 m range errors in the source-receiver offset can make the electric fields appear stronger or weaker than expected.

**Case study.** We conducted a pilot study of the CSEM method for gas-hydrate detection at Hydrate Ridge, offshore Oregon, in August 2004. This region has been extensively studied by ODP Leg 204 and has 3D seismic coverage, providing us with supporting background data for the EM technique. Figure 5 outlines our first results from an in-line CSEM data set, presented in pseudosection form (a technique widely used on land for dc resistivity and IP methods). Two transmission frequencies are shown (5 and 15 Hz). The 15-Hz pseudosection is sensitive to shallower sediments because of the shorter EM penetration depths, and this is reflected by a general agreement with the top of the 5-Hz pseudosection. Lateral changes in resistivity are well imaged with the pseudosection projection method. In regions where little or no hydrate is thought to exist (as in the basin at s18–s25) we observe more conductive (red) features, and in regions where more hydrate is expected we observe more resistive features (blue) (as on the summit at s4–s17). It seems possible that horizons B and B', highly faulted, coarse-grained, and/or volcanic ash-rich horizons which show high resistivities in logging while drilling, are being imaged in the 5-Hz data under s8–s15. Two anomalous regions exist, a highly resistive feature to the west (s1–s5) and a conductive feature projecting from s6. The resistive feature is consistent with a seismic inversion by Zhang et al. (2003), who inferred that this region contains higher hydrate and free-gas saturations. The conductive feature projecting from s6 could be a result of the receiver sitting directly over a conductor, such as a brine, or it could be that horizon A, a

highly porous ash-lined conduit which transports methane gas to the summit of Hydrate Ridge, is conductive as a result of the high porosity. Clearly, there are other lithologic features we are imaging such as the anticline observed beneath s15–s18 shown in the 5-Hz data. This feature is barely seen in the 15-Hz data, suggesting that it is deep.

The pseudosection projection method is better at imaging lateral resistivity variations than those with depth. To obtain true depth, a 2D inversion will be required. However, simple 1D inversions may be appropriate for the basin region (s19–s23). Depth estimates for this region suggest the sensitivity to sediments is in the top 300 m at 15 Hz and the top 500 m at 5 Hz. A rough estimate of hydrate or gas concentration can be done with a simple Archie's law calculation. Using Archie's parameters for nearby ODP Leg 204 well log data and CSEM-derived resistivities, we predict the hydrate concentration varies 0–30%. However, EM-derived concentrations are subject to any inaccuracies in Archie's equation and to our assumption of uniform values for the associated formation parameters.

**Hydrate concentrations.** There is a great need for laboratory studies of hydrate-bearing sediments to relate electrical conductivity to hydrate concentration. Stephen Kirby of the USGS stated at the Fall 2005 American Geophysical Union meeting that the gas-hydrate community receives a "D" for our understanding of laboratory properties of gas hydrates. To date, almost nothing is known about hydrate electrical resistivity except that hydrate behaves like an ice, which is electrically insulating. Laboratory studies of the relationship between electrical resistivity and hydrate concentration would put into context what we observe in the

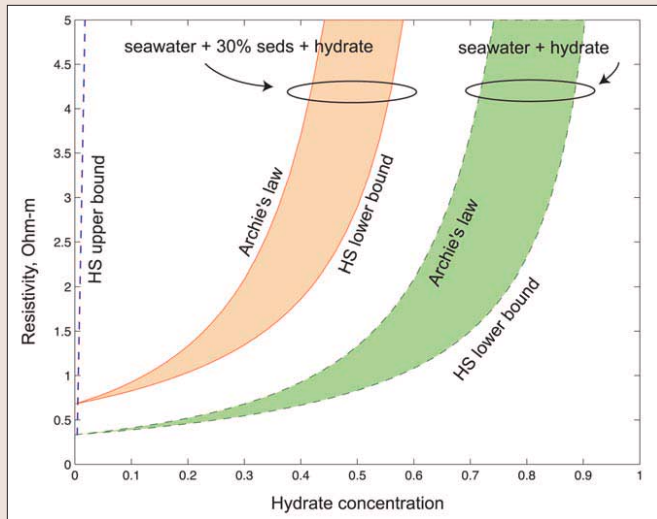


**Figure 6.** Archie's law, and Hashin-Shtrikman (HS) upper and lower bounds for a hydrate and seawater mix, and for a hydrate, seawater, and sediment mix. It is likely that the hydrate resistivity falls between Archie's law and the HS lower bound. The HS upper bound is unlikely to be a useful model but is included for completeness.

field and could provide a more accurate assessment of hydrate content.

In the absence of laboratory data, the standard approach has been to obtain hydrate concentration from Archie's law, but another useful method might be the Hashin-Shtrikman (HS) bounds. The HS lower bound is a theoretical minimum for the composite conductivity of resistive inclusions in a conductive matrix. This may be an appropriate model if hydrate forms as isolated granules within the sediment, as is often the case for disseminated hydrates. Figure 6 shows the predictions of Archie's law and the HS lower bound for a mix of hydrate and seawater and hydrate and seawater/sediment. At 10–20% concentration, the presence of hydrate has a modest but measurable effect on resistivity. At greater concentrations, the effect is dramatic no matter which model one chooses.

**Future directions.** The pilot study at Hydrate Ridge provided us with a useful data set for examining the application of CSEM to hydrate quantification. The importance of navigation is clear from the model studies and data. We can improve navigation of the seafloor receivers and transmitter by using a long baseline acoustic navigation system. The

transmission of higher frequencies will give us better resistivity images, provided that our navigation is sufficiently accurate at short ranges. We did attempt a towed system much like Edwards' (1997), but data could not be collected because of a technical failure. However, we plan to augment future surveys with this additional capability, since this data set will be more sensitive to the shallower section because of the shorter source-receiver offset. We plan to perform additional case studies and ground-truthing to develop a knowledge base of hydrate EM responses.

Furthermore, the extension of surveys into 3D is necessary, and it follows that data inversions in 2D and 3D are required as we develop these capabilities. It may be possible that EM methods are the best tools for obtaining a bulk assessment of hydrate content in a region. However, showing that the EM method is sensing bulk hydrate distribution may be difficult, since there is no way to predict hydrate using other geophysical methods. Adding magnetotelluric (MT) data to a CSEM survey may provide background resistivity on which to base our interpretations.

**Conclusions.** Electromagnetic methods for hydrate detection are certainly feasible. More field trials and laboratory studies will indicate how well this technique will work in practice to provide an assessment of the hydrate content and reduce the geohazard risk associated with gas hydrates.

**Suggested reading.** "First results from a marine controlled-source electromagnetic survey to detect gas hydrates offshore Oregon" by Weitemeyer et al. (*Geophysical Research Letters*, 2006). "Marine gas hydrate electromagnetic signatures in Cascadia and their correlation with seismic blank zones" by Schwalenberg et al. (*First Break*, 2005). "Three-dimensional distribution of gas hydrate beneath southern Hydrate Ridge: constraints from ODP Leg 204" by Tréhu et al., (*Earth Planetary Science Letters*, 2004). "Marine electromagnetic methods—a new tool for offshore exploration" by Constable (*TLE*, 2006). "Elastic inversion for distribution of gas hydrate, with emphasis on structural controls" by Zhang and McMechan (*Journal of Seismic Exploration*, 2006). **TJE**

*Acknowledgments:* The Scripps Institution of Oceanography Seafloor Electromagnetic Methods Consortium provides general funding for this research. Funds for ship time were provided by ExxonMobil and GERD, Japan. Thanks are extended to the Captain and Crew of the R.V. New Horizon and the technicians and engineers of the SIO marine EM Laboratory.

Corresponding author: kweiteme@ucsd.edu